

Low Frequency Observations of the 4 December 2021 Solar Eclipse

Whitham D. Reeve

1. Introduction

A total solar eclipse took place at high latitude in the southern hemisphere on 4 December 2021. The eclipse shadow passed over Union Glacier on Antarctica and the adjacent Weddell Sea. An attempt was made to observe the eclipse at low frequencies from a location over 16 thousand km away in the northern hemisphere at Cohoe Radio Observatory (CRO) in southcentral Alaska (figure 1).

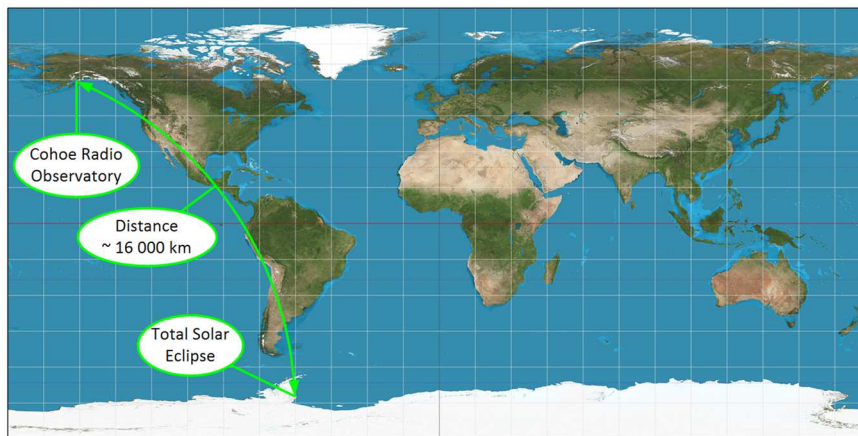


Figure 1 ~ Map showing location of Cohoe Radio Observatory in the northern hemisphere with respect to the point of greatest eclipse in the southern hemisphere on 4 December 2021. Underlying image source: GIS StackExchange

Although it is known that solar eclipses can affect low frequency radio propagation, it was not known what effects, if any, this eclipse would have on propagation paths widely separated from the eclipse path. To try to find out, I recorded and analyzed the received signals from three radio transmitters in the *very low frequency* (VLF, 3 to 30 kHz) and *low frequency* (LF, 30 to 300 kHz) bands. The recordings covered time periods before, during and after the 4 December eclipse.

I did not expect to observe perturbed propagation because of the distances involved, and the results described in section 4 are inconclusive. However, I was interested in determining and learning about reliable sources of relevant eclipse data and the analytic procedures and radio observation techniques that might be specific to eclipses. This article briefly discusses low frequency radio propagation (section 2), eclipse characteristics (section 3), results of the observations (section 4), discussion of the results (section 5) and the instrumentation and setups (section 6). This information sets the stage for observations of future eclipses.

2. Brief Overview of Low Frequency Propagation & Propagation Path Characteristics

The low frequency signals of interest here propagate in the spherical Earth-ionosphere waveguide in which the ionosphere forms the upper boundary and Earth's surface forms the lower boundary of the waveguide. Under normal diurnal conditions, the ionosphere's D-region changes height in response to solar radiation. During the day, the D-region is lower and radio waves with frequencies in the tens of kilohertz range encounter more absorption leading to lower received signal levels. At night, the D-region rises (or disappears) and the radio

waves encounter less absorption leading to higher received signal levels. For a more detailed discussion on VLF propagation, see [{Reeve19-1}](#)

During normal conditions, daily plots of the signal power received from a given distant low frequency transmitter show a characteristic pattern. However, the D-region electron density in the shadow of a solar eclipse decreases, thus temporarily affecting radio waves passing through it and disturbing the characteristic pattern. Thus, observing an eclipse at low frequencies may show variations in the duration and timing due to perturbances along the propagation paths.

Low frequency signals can follow a direct great circle path from the transmitter to receiver, called *short path*. Because low frequency signal attenuation in the Earth-ionosphere waveguide is so low, the signals also may propagate on a longer great circle path in the opposite direction, called *long path*. Other paths are possible because of the spherical nature of the waveguide and land, water and ice interfaces along the way. Because of the many possible propagation modes, a given location can experience destructive or constructive interference that varies over time and with propagation conditions.

The great circle propagation paths to CRO from only four transmitter stations, out of 12 to 15 that are receivable at CRO, intersected or nearly intersected the eclipse path (table 1). Three of the four transmitter stations, JJI, NLK and WWVB, are located in the northern hemisphere. All propagation path intersections, or near intersections, occurred only on the long paths and early in the eclipse event.

Table 1 ~ Transmitter stations and path characteristics. All distances and azimuths are with respect to Coho Radio Observatory (CRO). The long path distances are determined by first calculating the short path distances and subtracting the result from 40 000 km, Earth’s approximate circumference. Station key: NWC: North West Cape, Australia; JJI: Ebino, Miyazaki, Japan; NLK: Washington, USA; WWVB: Colorado, USA (a receiver was not setup for WWVB on this eclipse).

Station	Frequency (kHz)	Short Path distance (km)	Short path azimuth (° TN)	Long path distance (km)	Geographical Coordinates	Remarks
NWC	19.8	12 350	263	27 650	21.816° S, 114.166° E	
JJI	22.2	6 299	277	33 701	32.076° N, 130.829° E	
NLK	24.8	2 308	113	37 792	48.203° N, 121.917° W	
WWVB	60.0	3 818	104	36 182	40.678° N, 105.047° W	Rx not setup
CRO	RX	NA	NA	NA	60.368° N, 151.315° W	For reference

For the eclipse on 4 December 2021, CRO was on Earth’s nightside with partial illumination of the short and long paths during the eclipse time period. Mercator projection plots show the solar terminator and propagation paths for the time of greatest eclipse (0735 UTC) (figure 2). The solar terminator moves east-to-west as the Sun moves across the sky. Note that the long paths and early edges of the eclipse shadow are close to the solar terminator.

Earth’s magnetic field influences radio propagation, so I considered both the magnetic coordinates of the point of greatest eclipse and the conjugate of those coordinates. The geographic coordinates of the greatest eclipse location were 76° 46.7’ S, 46° 11.9’ W. The conjugate point is determined by first calculating the geomagnetic coordinates of the greatest eclipse geographic location, taking the conjugate of the geomagnetic coordinates and then converting the conjugate to geographic coordinates for plotting purposes.

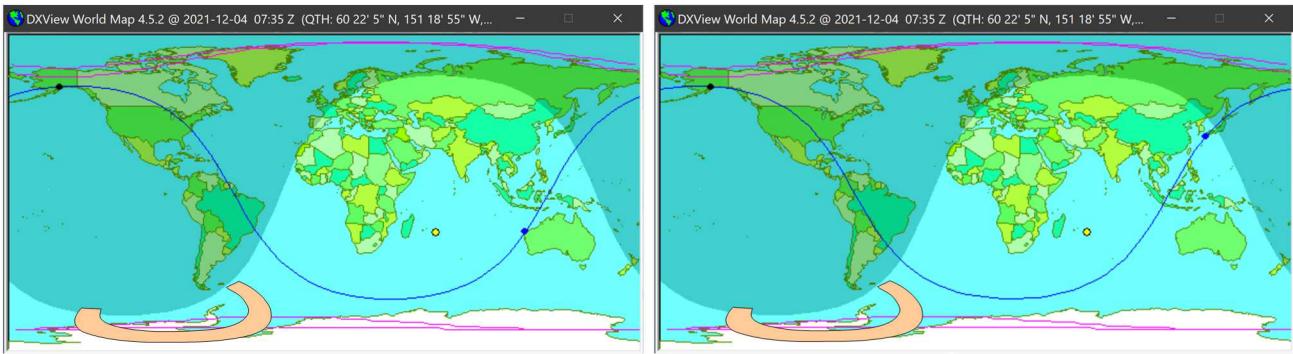


Figure 2.a ~ Solar terminator near time of greatest eclipse and short and long paths for transmitter stations NWC in Australia, 19.8 kHz (left) and JJI in Japan, 22.2 kHz (right). The path of total eclipse is shown in the lower-left corner as a tan arc. Areas of partial eclipse cover a much larger area, primarily over Antarctica. Underlying plots from {DXView} software

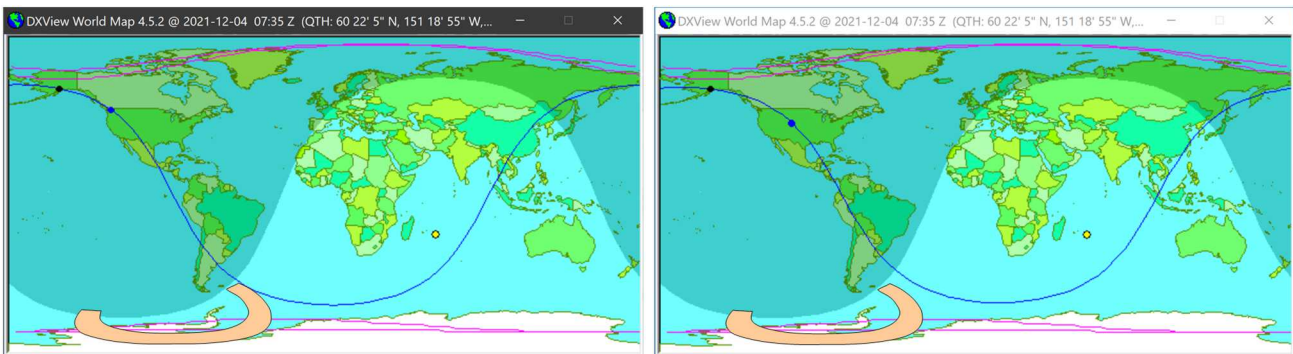


Figure 2.b ~ Solar terminator near time of greatest eclipse and short and long paths for transmitter stations NLK in Washington USA, 24.8 kHz (left) and WWVB in Colorado USA, 60 kHz (right). The path of total eclipse is shown in the lower-left corner as a tan arc. The long path from station NLK comes closest to the total eclipse path. Areas of partial eclipse cover a much larger area, primarily over Antarctica. Underlying plots from {DXView} software

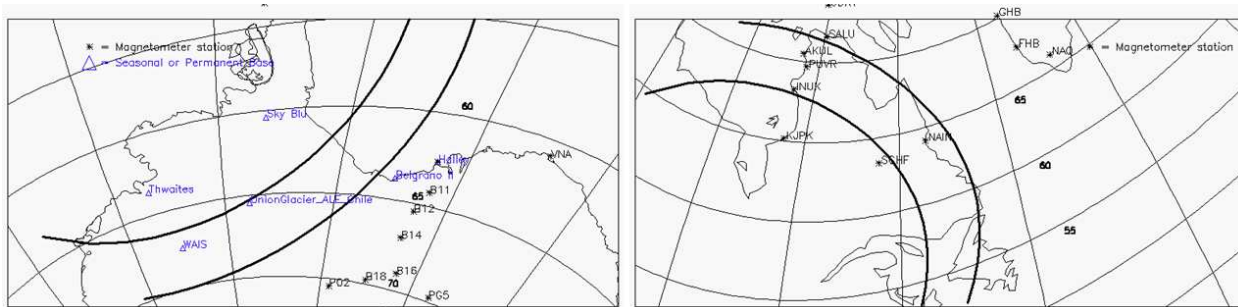


Figure 3 ~ Sketches of the actual eclipse path over Antarctica (left) and the magnetic conjugate path over northeastern Canada (right). Source: Unknown

The geomagnetic coordinates calculated from {Kyoto} of the greatest eclipse location are 67.88° S, 15.81° E, and the conjugate coordinates are 67.88° N, 15.81° E. Conversion of the conjugate geomagnetic coordinates to geographic coordinates, again from {Kyoto}, gives $58^\circ 53.76'$ N, $61^\circ 16.92'$ W. This is located near the coast of Newfoundland and Labrador and the Labrador Sea. These coordinates are for a single point; the conjugate path follows an arc across northwestern Canada. Sketches show the eclipse paths at both locations (figure 3).

Comparison to the solar terminator plots shows that none of the radio propagation paths were near the conjugate path.

3. Eclipse Characteristics

The greatest eclipse was reached at approximately 0735 UTC (10:35 pm Alaska Standard Time). The Sun was fully eclipsed for about 1 h (0700 to 0806) and partially eclipsed for about 4 h (0529 to 0937 UTC).

The Sun and eclipse path characteristics are summarized by NASA's Goddard Space Flight Center (figure 4). An animation of the eclipse may be seen at [{NASA-AN}](#). Additional eclipse information and graphics are available at [{TD4Dec}](#) including a color-graduated image of the partial and total eclipse regions (figure 5).

4. Observations

The received signals from stations NWC (19.8 kHz), JJI (22.2 kHz) and NLK (24.8 kHz) were sampled and recorded at 15 s intervals for 3 d before, day of and 3 d after the eclipse (instrumentation is described in section 6). The extended time period was implemented to establish daily signal patterns unaffected by the eclipse that could be compared to the day of the eclipse. Signal data plots are shown for each of the three stations for the 7-day period (figure 6) as well as a combined plot of the three stations on the day of the eclipse (figure 7). Shaded areas on the plots indicate local darkness (sunset to sunrise) at CRO.

Regular signal level variations are observed due to sunrise and sunset along the propagation paths. The times and specific details of these variations depend on, among other things, the location of the transmitter and receiver stations with respect to the moving solar terminator.

The plots include a solid gold vertical arrow that marks the time of the greatest eclipse (0735 UTC), and dashed gold arrows that show the same time of day as the eclipse but on the days before and after the eclipse. The dashed arrows are used to establish a reference signal time pattern for comparison to the eclipse time.

Sunset at Coho on 3 December was 0104 UTC (4:04 pm local time on 3 December), about 6.5 h before the eclipse. The following sunrise was 1849 UTC (9:49 am local time on 4 December), approximately 11 h after the eclipse. Therefore, the local Coho sunrise and sunset were outside the time of the eclipse event. Coho is at geographic latitude 60° N and the daylight hours are short during December, lasting only 6.25 h on eclipse day. Referring to the solar terminator plots above, the short and long radio propagation paths cross the solar terminator in various ways (table 2).

Total Solar Eclipse of 2021 Dec 04

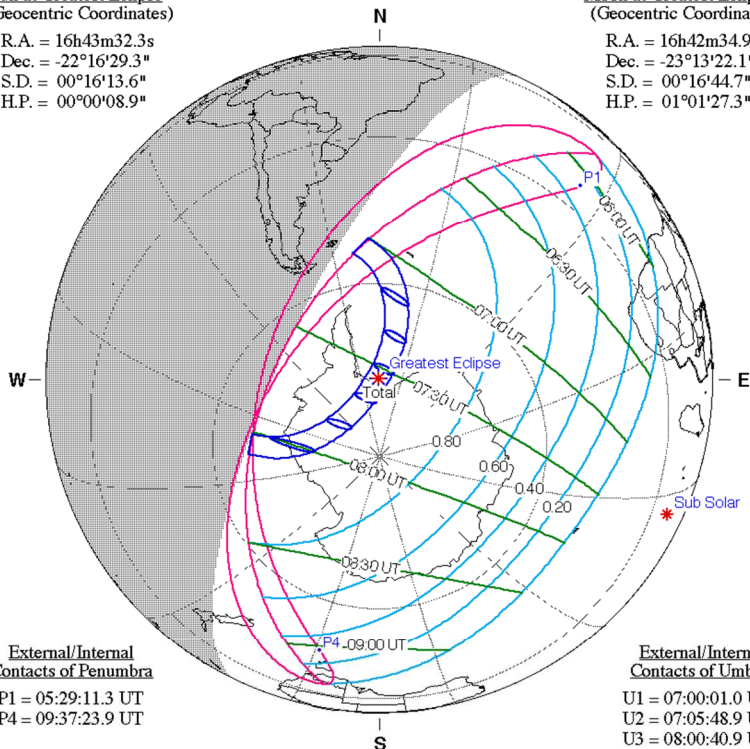
Geocentric Conjunction = 07:56:04.9 UT J.D. = 2459552.830612
 Greatest Eclipse = 07:33:22.5 UT J.D. = 2459552.814844
 Eclipse Magnitude = 1.0367 Gamma = -0.9526
 Saros Series = 152 Member = 13 of 70

Sun at Greatest Eclipse
(Geocentric Coordinates)

R.A. = 16h43m32.3s
 Dec. = -22°16'29.3"
 S.D. = 00°16'13.6"
 H.P. = 00°00'08.9"

Moon at Greatest Eclipse
(Geocentric Coordinates)

R.A. = 16h42m34.9s
 Dec. = -23°13'22.1"
 S.D. = 00°16'44.7"
 H.P. = 01°01'27.3"



External/Internal
Contacts of Penumbra

P1 = 05:29:11.3 UT
 P4 = 09:37:23.9 UT

External/Internal
Contacts of Umbra

U1 = 07:00:01.0 UT
 U2 = 07:05:48.9 UT
 U3 = 08:00:40.9 UT
 U4 = 08:06:29.2 UT

Local Circumstances at Greatest Eclipse

Lat. = 76°46.7'S Sun Alt. = 17.2°
 Long. = 046°11.9'W Sun Azm. = 114.8°
 Path Width = 418.6 km Duration = 01m54.4s

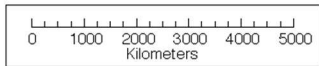
Ephemeris & Constants

Eph. = Newcomb/ILE
 ΔT = 78.8 s
 k1 = 0.2724880
 k2 = 0.2722810
 Δb = 0.0" Δl = 0.0"

Geocentric Libration
(Optical + Physical)

l = -0.23°
 b = 1.26°
 c = 6.09°

Brown Lun. No. = 1224



F. Espenak, NASA's GSFC - Fri, Jul 2,
sunearth.gsfc.nasa.gov/eclipse/eclipse.html

Figure 4 ~ Detailed characteristics of the 4 December eclipse. The asterisk at the center of the map marks the point on Earth's surface nearest to the axis of the Moon's shadow at greatest eclipse. The blue arcs indicate the extent of the greatest eclipse with oblong marks at 10-minute intervals. The looped magenta lines show the extent of the Moon's shadow nearest to the sunrise/sunset line (solar terminator). The cyan lines indicate the path of the Moon's shadow with green time marks at 30-minute intervals. The times of first and last contacts of the partial eclipse shadow (penumbra) are indicated by P1 and P2 and the times of the contacts of the total eclipse (umbra) are indicated by U1 through U4. The definitions of other details in this image can be found at [{NASAKey}](#). Image source: NASA GFSC [{NASA4Dec}](#)

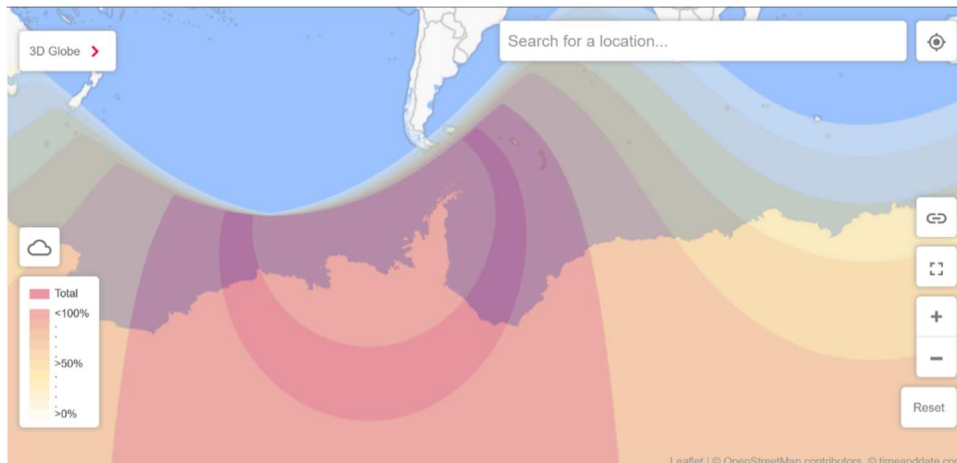


Figure 5 ~ Map showing the extent of total and partial eclipse areas, indicated on the color scale in the lower-left corner. Comparison with the solar terminator maps above indicates that the propagation long paths of the three stations NWC, JJI and NLK cross areas of partial eclipse. Image source {TD4Dec}.

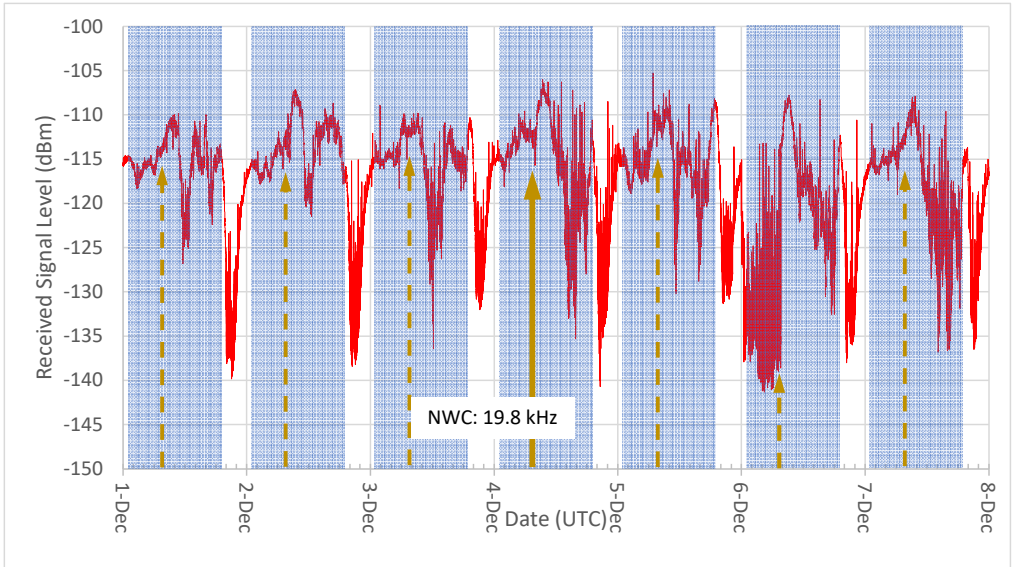


Figure 6.a ~ NWC (19.8 kHz). The daily patterns show approximately 25 dB signal level decrease for a few hours during the local Cohoe morning. The station apparently was off-the-air for several hours on 6 December. A minor signal level dip before peak occurs around 0100 and 0800 each day, possibly due to sunrise or sunset along the paths.

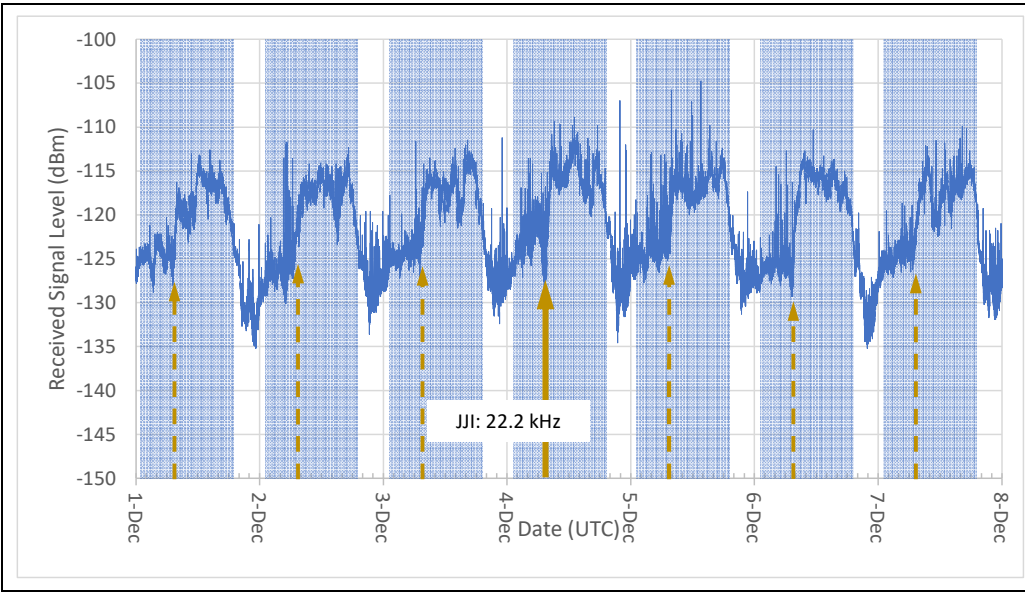


Figure 6.b ~ Station JJI (22.2 kHz). The daily patterns are similar to NWC except that the daytime signal level dip is approximately 20 dB and the only dip occurs on eclipse day; all other days show a relatively sharp increase in received signal level.

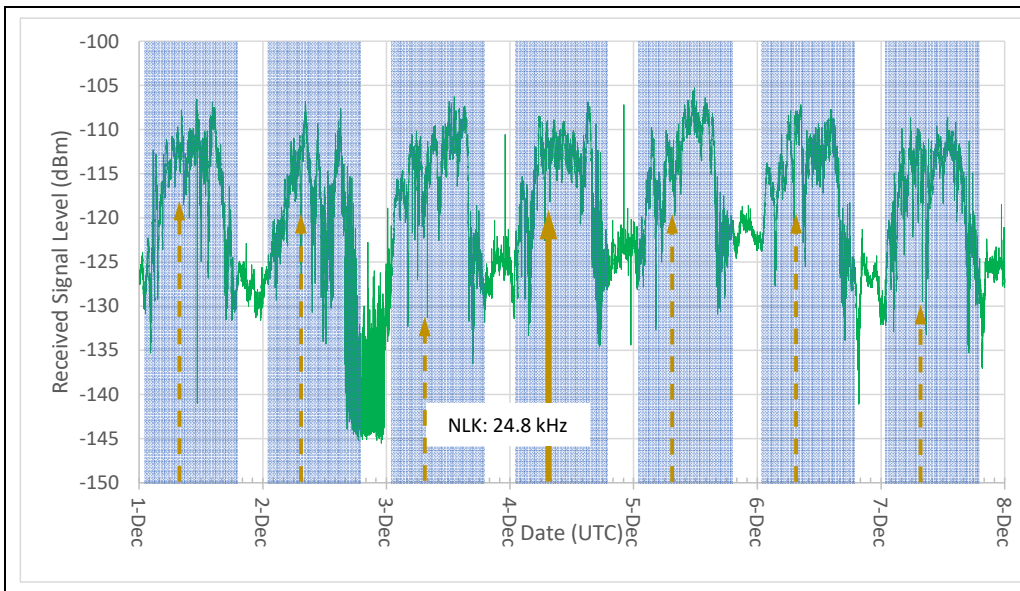


Figure 6.c ~ Station NLK (24.8 kHz). The daytime (Cohoe) signal levels decrease about 15 dB with no obvious change in signal patterns on eclipse day. An apparent outage occurred late in the UTC day 2 December.

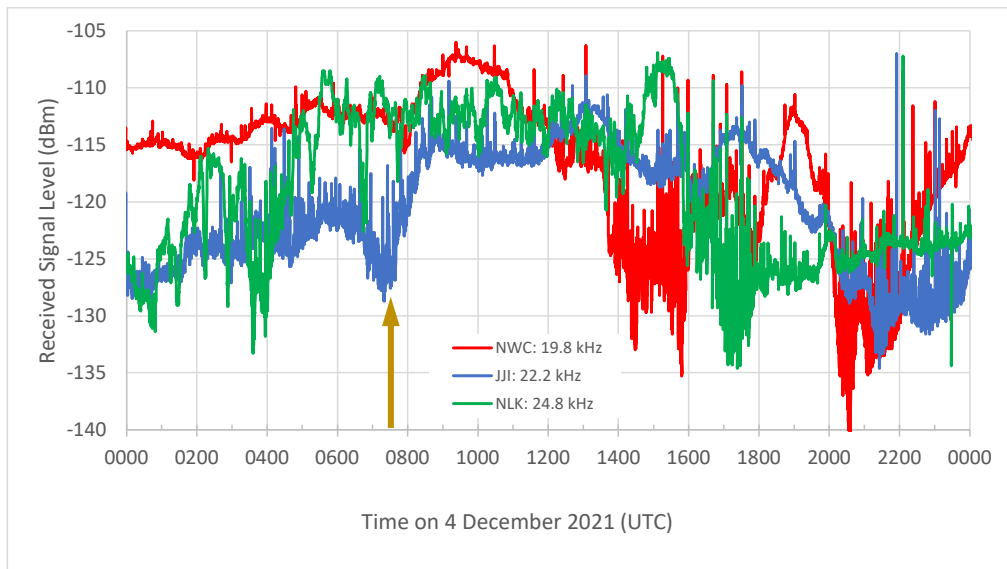


Figure 7 ~ Combine plot of all three stations on eclipse day. Stations NWC (red trace) and JJI (blue trace) show an anomaly at the time of greatest eclipse, lasting roughly 1 h and indicated by the gold arrow. The minimum of the dip of the NWC signal occurs about 30 min later than JJI.

Table 2 ~ Solar terminator crossings of short and long propagation paths

Station (Frequency)	Short Path Crossing	Long Path Crossing
NWC (19.8 kHz)	Yes, once	Yes, once
JJI (22.2 kHz)	Yes, once	Yes, once
NLK (24.8 kHz)	No	Yes, twice

The received signal plots broadly show the expected daily signal variations – signal increase at night and signal decrease during the day with various dips and peaks, and ramp-ups and ramp-downs depending on the path and time of day. Stations NWC (19.8 kHz) and JJI (22.2 kHz) show a relatively slow signal ramp-up for a few hours after local sunset followed by a much quicker ramp-up near the middle of the local night. The received signal levels then dip before rising again. A deep dip occurs near local sunrise. The short path propagation direction from these two stations is west-to-east. Station NLK (24.8 kHz) with east-to-west propagation shows a somewhat different pattern but the local daytime signal reduction still is obvious.

5. Discussion

It is reasonable to assume that eclipse effects could be observed not only during the time period of total eclipse but also during the partial eclipse periods – any time the radio path passes through or near the eclipse shadow – so the main period of interest runs at least from 0529 to 0937 UTC.

The two eastern transmitters, NWC in Australia and JJI in Japan, show a distinct dip in the received signal level during the time period of total eclipse. The signal from station JJI starts to decrease at about 0600 and has fully recovered by 0800. The dip in the signal from NWC is not as pronounced and occurs at 0800, approximately 30 min after JJI. For comparison, in the brief analysis of the annular solar eclipse over northeastern Canada on 10 June 2021 ([Reeve21](#)), anomalous signal levels at eclipse time compared to the days surrounding the eclipse were noted on the radio path from station NPM (21.4 kHz) in Hawaii to CRO.

Concluding that these eclipses clearly affected the received signals requires too much imagination and no such conclusion is made here. It remains to be seen if studies of future eclipses reveal a similar pattern.

On the other hand, the effort was successful in terms of procedure development and data reduction and these methods will be used during the future eclipses listed in table 3. It should be no surprise that one of the most important and useful information sources is NASA at [{NASA-SE}](#). I also found the graphics on [{TimeDate}](#) very useful and in some ways easier to use than the much broader range of technical data available from NASA. Section 7 lists these references as well as the specific webpages used for the 4 December eclipse and other useful websites.

Table 3 ~ Solar eclipses 2022 through 2024 (source: [{NASA-DEC}](#))

Date	Type	Hemisphere	Remarks
30 April 2022	Partial	Southern	Same general area as 4 Dec 2021 eclipse
25 October 2022	Partial	Northern	
20 April 2023	Hybrid	Primarily southern	Crosses equator near end
14 October 2023	Annular	Primarily northern	Crosses equator near end
8 April 2024	Total	Primarily northern	Crosses equator near beginning
2 October 2024	Annular	Primarily southern	Crosses equator near beginning

Radio observation techniques and procedures are described in section 6. Most of these were developed over several years of observations with software defined radio (SDR) receivers and both a shop-built and a refurbished commercial loop antenna at Coho Radio Observatory.

Although the time-frequency station WWVB (60 kHz) in Colorado was mentioned in section 2, the square loop antenna used for the observations is not usable at 60 kHz and a receiver was not setup for that station. However, a dedicated loop antenna designed for 60 kHz and an SDR receiver will be setup for future eclipses. The additional data will be integrated and analyzed in the same manner as described here.

6. Instrumentation

The major components at Cohoe Radio Observatory used in the above-described observations were a shop-built square loop antenna, an SDRPlay *RSPduo* SDR receiver and a Lenovo small form factor PC running Windows 10. The square loop is an untuned passive antenna preset to an east-west azimuth. *SDRuno* software, which is native to the SDRPlay SDR products, was used to gather received signal level data. A block diagram shows the basic setup (figure 8). More observatory details are given at [Reeve19-2](#).

I setup three virtual receivers in *SDRuno*, VRX-00, VRX-01, and VRX-02, for the frequencies 19.8, 22.2 and 24.8 kHz, respectively. All virtual receivers ran continuously over the 7-day study period, 3 days before the eclipse (1 December start), eclipse day (4 December) and 3 days after the eclipse (7 December stop). I used the *PWR & SNR to CSV* function to save the measured signal level every 15 seconds to Comma Separated Variable (.csv) files, one file for each virtual receiver. At the end of the observations, the CSV files were uploaded to a PC in the Anchorage Radio Observatory for post-processing and plotting. All plots were produced with Excel.

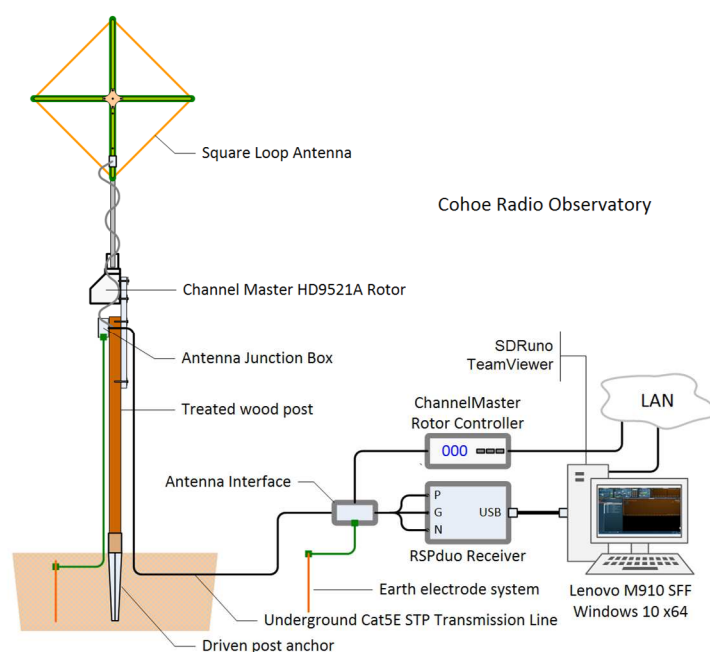


Figure 8 ~ Block diagram of square loop antenna, SDRduo receiver and PC setup at Cohoe Radio Observatory. Not shown are the observatory support infrastructure such as dc power supplies, local area network equipment, NTP time server and uninterruptible power system. The loop antenna diagonal dimension is 1.2 m, and its center is 3.4 m above ground level. The balanced high-impedance (HI-Z) antenna input of the receiver is connected to the antenna through Cat5E STP DB (direct burial) cable. The antenna mast is mounted on a simple TV antenna rotator that is controlled through a web browser. The antenna was set to east-west (090-270° TN) azimuth for the eclipse study. Image © 2021 W. Reeve

The main spectrum and waterfall displayed by *SDRuno* shows all received signals within the configured frequency span (figure 9). For the measurements discussed in this article, the receiver was set to Zero Intermediate Frequency (ZIF) mode with a sample rate of 2 MHz and factor 32 decimation. These settings provide 62.5 kHz maximum displayed frequency span and FFT frame size of 65 536. In this configuration, the available resolution bandwidth (RBW) settings were 0.95, 1.91, 3.81, 7.63, 15.26 and 30.52 Hz. A low RBW was not necessary for the study, so it was set to 7.63 Hz as a tradeoff between resolution and displayed noise floor smoothness.

In the ZIF mode, the receiver local oscillator (LO) offset can be set automatically by the *SDRuno* software. I enabled this feature, which provided an LO of 3900 Hz and an initial displayed frequency range of -27.35 to

+35.15 kHz. I then used the 4x zoom function to reduce the displayed span to 15.6 kHz and adjusted it to show the range 14.7 to 30.3 kHz.

The receiver IF gain was set to Auto, and the RF gain was set to maximum. It should be noted that the IF and RF gains and the methods for setting them were far from optimized in early versions of the SDRPlay hardware and software. However, SDRPlay made incremental improvements over time so that they now work in a conventional manner. No Noise Reduction (NR) or Noise Blanker (NB) was used. Although not relevant to this study, the demodulation mode was set to CW with 700 Hz offset and 150 Hz bandwidth.

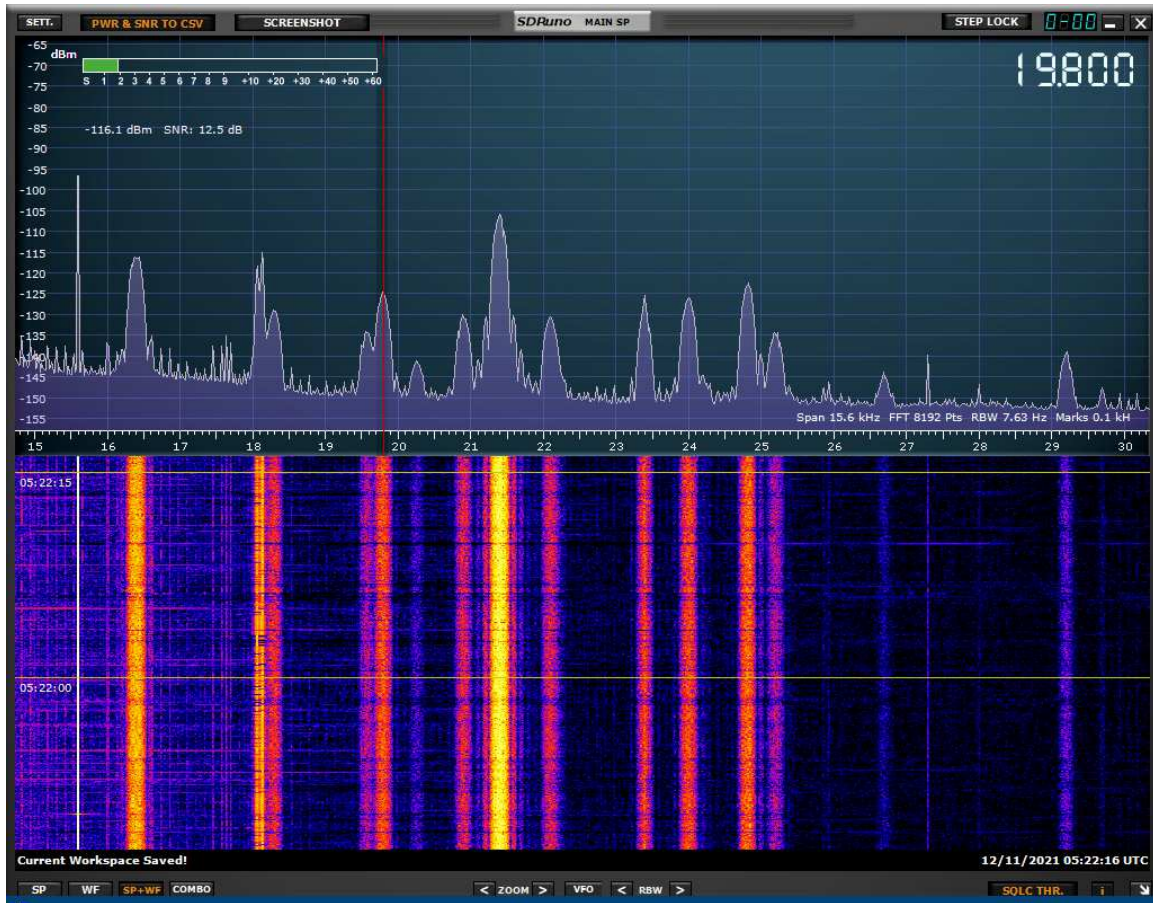


Figure 9 ~ Spectrum and waterfall for 11 December 2021 (a week after the eclipse) showing receiver tuned to the NWC station on 19.8 kHz and with the loop antenna oriented east-west. The tuning is marked by the red vertical line in the upper panel. The span is 15.6 kHz with 7.63 Hz resolution bandwidth. Many VLF signals are present including JJI (22.2 kHz) and NLK (24.8 kHz). Note that JJI is very weak and almost hidden behind a stronger signal at 22.1 kHz. The strongest signal at the time of this image is station NPM in Hawaii USA at 21.4 kHz. Other signals are (with presumed station ID in parentheses, see [{VLFStaLst}](#)): 16.4 (JXN), 18.1 (RDL), 18.3 (HWU), 19.6 (GBZ), 20.3 (ICV), 20.9 (HWU), 23.4 (DHO38), 24.0 (NAA), 24.8 (NLK), 25.2 (NML), 26.7 (TBB), and 29.2 (Unknown) kHz. The very narrow spectrum spikes are spurious signals including harmonics of 60 Hz powerline interference. Image from SDRuno.

7. References & Weblinks

{[Reeve19-1](#)} Reeve, W., Monitoring Low Frequency Propagation with a Software Defined Radio Receiver, Part I ~ Concepts, 2019, available at:

http://www.reeve.com/Documents/Articles%20Papers/Propagation/Reeve_LFProp-ConceptsP1.pdf

{Reeve19-2} Reeve, W., Monitoring Low Frequency Propagation with a Software Defined Radio Receiver, Part II ~ Observations, 2019, available at:

http://www.reeve.com/Documents/Articles%20Papers/Propagation/Reeve_LFProp-ObsvP2.pdf

{Reeve21} Reeve, W., Comparison of Signals from South and West VLF Stations During June 2021, available at: https://reeve.com/Documents/Articles%20Papers/Reeve_Comp_VLFSta_Jun2021_SARA.pdf

{DXView} <http://www.dxlabsuite.com/dxview/>

{Kyoto} <http://wdc.kugi.kyoto-u.ac.jp/igrf/gggm/>

{NASA4Dec} <https://eclipse.gsfc.nasa.gov/SEplot/SEplot2001/SE2021Dec04T.GIF>

{NASA-AN} <https://eclipse.gsfc.nasa.gov/SEanimate/SEanimate2001/SE2021Dec04T.GIF>

{NASA-DEC} <https://eclipse.gsfc.nasa.gov/SEdecade/SEdecade2021.html>

{NASA-SE} <https://eclipse.gsfc.nasa.gov/>

{NASAKey} <https://eclipse.gsfc.nasa.gov/SEplot/SEplotkey.html>

{TD4Dec} <https://www.timeanddate.com/eclipse/globe/2021-december-4>

{TimeDate} <https://www.timeanddate.com/eclipse/>

{VLFStaLst} https://reeve.com/Documents/Articles%20Papers/Reeve_VLF-LFStationList.pdf



Author: Whitham Reeve obtained B.S. and M.S. degrees in Electrical Engineering at University of Alaska Fairbanks, USA. He worked as a professional engineer and engineering firm owner/operator in the airline and telecommunications industries for more than 40 years and now manufactures electronic equipment used in radio astronomy. He also is a part-time space weather advisor for the High-frequency Active Auroral Research Program (HAARP) and a member of the HAARP Advisory Committee. He has lived in Anchorage, Alaska his entire life. Email contact: whitreeve@gmail.com

Document Information

Author: Whitham D. Reeve

Copyright: © 2022 W. Reeve

Revisions: 0.0 (Original draft started, 07 Jul 2021)
0.1 (Added stations table, 07 Nov 2021)
0.2 (Added data plots, 10 Dec 2021)
0.3 (Added discussion, 13 Dec 2021)
0.4 (Minor cleanup, 27 Dec 2021)
0.5 (Expanded discussion, 29 Dec 2021)
0.6 (Completed 1st draft, 02 Jan 2022)
0.7 (Final edits for distribution, 31 Jan 2022)

Word count: 3601

File size (bytes): 8830847